New Insights into the Berg−Holm Oxomolybdoenzyme Model

Christian J. Doonan,[1a] Damian A. Slizys,[1b] and Charles G. Young*,[1a]

Contribution from the School of Chemistry, University of Melbourne, Parkville, Victoria 3052, Australia, and Department of Medicinal Chemistry, Victorian College of Pharmacy, Monash University, Clayton, Victoria 3168, Australia

Received January 11, 1999

Abstract: Reaction of MoO_2(L-NS_2) [L-NS_2 = 2,6-bis(2,2-diphenyl-2-thioethyl)pyridinate(2−)] with PPh_3 in *N*,*N*-dimethylformamide (dmf), chloroform, or mixtures thereof results in the formation of purple, dinuclear, μ-oxo-Mo(V) compounds, Mo_2O_3(L-NS_2)$_2$·2sol (sol = dmf, $CHCl_3$, or mixtures thereof), which can be dried at 80 °C under vacuum to give Mo_2O_3(L-NS_2)$_2$. ^{31}P NMR experiments were consistent with the following reaction: $2Mo^{VI}O_2$(L-NS_2) + PPh_3 → $Mo^{V}_2O_3$(L-NS_2)$_2$ + $OPPh_3$. The compounds have been characterized by microanalysis, IR, and UV−visible spectroscopy, electrospray ionization mass spectrometry, and X-ray diffraction studies of Mo_2O_3(L-NS_2)$_2$·2dmf and Mo_2O_3(L-NS_2)$_2$·2$CHCl_3$. Dinuclear Mo_2O_3(L-NS_2)$_2$ is comprised of five-coordinate, trigonal-bipyramidal Mo centers bridged by a strictly linear Mo−O−Mo unit with Mo−O = 1.8639(6) Å for the dmf disolvate [1.8703(4) Å for the $CHCl_3$ disolvate]. Each Mo center is further coordinated by a tridentate L-NS_2 ligand and a terminal oxo ligand (Mo═O = 1.681(5) Å [1.696(4) Å]). The [Mo_2O_3] core is planar, and the terminal oxo ligands adopt an anti disposition. These findings provide new insights into the oxomolybdoenzyme model first described by Berg and Holm (Berg, J. M.; Holm, R. H. *J. Am. Chem. Soc.* **1985**, *107*, 917 and 925; Craig, J. A.; Holm, R. H. *J. Am. Chem. Soc.* **1989**, *111*, 2111 and references therein), viz., (i) mononuclear $Mo^{IV}O$(L-NS_2)(dmf) is not the product of the aforementioned reaction in dmf or mixed solvents, and (ii) comproportionation and dinucleation, rather than being absent, are defining reactions in the oxygen atom transfer chemistry of this system.

Introduction

A number of very important models for the oxomolybdoenzymes have been reported by Holm and co-workers.[2−16] The first, originally reported by Berg and Holm,[2−4] featured oxomolybdenum complexes of the 2,6-bis(2,2-diphenyl-2-thioethyl)pyridinate(2−) ligand, L-NS_2. These were designed to suppress comproportionation and the formation of biologically irrelevant μ-oxo-Mo(V) species during oxygen atom transfer (OAT) reactions involving mononuclear complexes of Mo(VI) and Mo(IV). The synthesis and characterization of orange $Mo^{VI}O_2$(L-NS_2) and purple $Mo^{IV}O$(L-NS_2)(dmf) (dmf = *N*,*N*-dimethylformamide), the "mononuclear" components of the model, were communicated in 1984.[2] Subsequent papers[3−8] and reviews[9,10] reported detailed kinetics studies of stoichiometric and catalytic OAT reactions (including several involving biological substrates), the coupling of these reactions to the reduction of MoO_2(L-NS_2) to MoO(L-NS_2)(dmf) by thiols, and thermochemical assessments of the reactions. Two very significant claims were made with respect to this model:[2−10] (i) OAT involved mononuclear Mo(VI) and Mo(IV) complexes and was *not* accompanied by detectable comproportionation or the formation of dinuclear μ-oxo-Mo(V) species, and (ii) the model represented the first "steric solution" to the comproportionation−dinucleation problem faced when developing valid models for the oxomolybdoenzymes. In this paper we provide important new insights into the celebrated and widely cited Berg−Holm model.

The dioxo-Mo(VI) component of the model, MoO_2(L-NS_2), has been characterized by microanalysis, IR, NMR, and UV−visible spectroscopy, and X-ray diffraction.[2,3] It is mononuclear and exhibits a distorted trigonal-bipyramidal structure with *cis* oxo and *trans* thiolate ligands. It reacts with PPh_3 in dmf to produce a purple compound characterized as MoO(L-NS_2)(dmf) on the basis of microanalysis and IR and UV−visible spectroscopy.[2,3] The formulation was also supported by a ^{31}P NMR experiment, consistent with the synthetic reaction shown in eq 1.[2,10]

$$Mo^{VI}O_2(\text{L-}NS_2) + PPh_3 + \text{dmf} \rightarrow Mo^{IV}O(\text{L-}NS_2)(\text{dmf}) + OPPh_3 \quad (1)$$

The purple compound has not been structurally characterized, and while there has been some discussion of a possible dinuclear

(1) (a) University of Melbourne. (b) Monash University.
(2) Berg, J. M.; Holm, R. H. *J. Am. Chem. Soc.* **1984**, *106*, 3035.
(3) Berg, J. M.; Holm, R. H. *J. Am. Chem. Soc.* **1985**, *107*, 917.
(4) Berg, J. M.; Holm, R. H. *J. Am. Chem. Soc.* **1985**, *107*, 925.
(5) Harlan, E. W.; Berg, J. M.; Holm, R. H. *J. Am. Chem. Soc.* **1986**, *108*, 6992.
(6) Caradonna, J. P.; Harlan, E. W.; Holm, R. H. *J. Am. Chem. Soc.* **1986**, *108*, 7856.
(7) Caradonna, J. P.; Reddy, P. R.; Holm, R. H. *J. Am. Chem. Soc.* **1988**, *110*, 2139.
(8) Craig, J. A.; Holm, R. H. *J. Am. Chem. Soc.* **1989**, *111*, 2111.
(9) Holm, R. H.; Berg, J. M. *Pure Appl. Chem.* **1984**, *56*, 1645.
(10) Holm, R. H. *Coord. Chem. Rev.* **1990**, *100*, 183.
(11) Gheller, S. F.; Schultz, B. E.; Scott, M. J.; Holm, R. H. *J. Am. Chem. Soc.* **1992**, *114*, 6934.
(12) Schultz, B. E.; Gheller, S. F.; Muetterties, M. C.; Scott, M. J.; Holm, R. H. *J. Am. Chem. Soc.* **1993**, *115*, 2714.
(13) Schultz, B. E.; Holm, R. H. *Inorg. Chem.* **1993**, *32*, 4244.
(14) Tucci, G. C.; Donahue, J. P.; Holm, R. H. *Inorg. Chem.* **1998**, *37*, 1602.
(15) Donahue, J. P.; Lorber, C.; Nordlander, E.; Holm, R. H. *J. Am. Chem. Soc.* **1998**, *120*, 3259.
(16) Donahue, J. P.; Goldsmith, C. R.; Nadiminti, U.; Holm, R. H. *J. Am. Chem. Soc.* **1998**, *120*, 12869.

10.1021/ja9900959 CCC: $18.00
Published on Web 06/26/1999

structure,[10,17] its formulation as an oxo-Mo(IV) complex has never been questioned.

However, many of the properties of the purple compound are inconsistent with its formulation as MoO(L-NS_2)(dmf). First, the purple color and associated UV−visible spectrum are typical of dinuclear μ-oxo-Mo(V) species.[18−21] Second, the reported ν(Mo═O) IR band at 945 cm^{-1} is low in energy for a mononuclear oxo-Mo(IV) complex and again is more typical of a μ-oxo-Mo(V) species.[18−20,22] Third, the observation of saturation kinetics in the reactions of the compound with oxygen atom donors is uncharacteristic of mononuclear oxo-Mo(IV) complexes.[11−13,23−27] The mechanistic interpretation of these kinetics invoked a preequilibrium displacement of dmf from MoO(L-NS_2)(dmf) by substrate XO ($K = (4-16) \times 10^3$), followed by O−X bond cleavage and concomitant OAT with rate constants $k = (1.4-1.7) \times 10^{-3}$ s^{-1}.[4−10] The lack of a significant substrate dependence in k is another unusual feature of the kinetics. Saturation kinetics are observed for OAT reactions involving μ-oxo-Mo(V) species, where the mechanism is proposed to involve the preequilibrium binding of the substrate at a vacant site on the dinuclear complex, followed by OAT via concerted O−X and (μ-O)−Mo bond cleavage.[25,28,29] Finally, comproportionation and dinucleation reactions are notable in molybdenum chemistry, and dinuclear, five- and six-coordinate, μ-oxo-Mo(V) complexes of the types $Mo_2O_3L_4$ (L = bidentate),[18,19,30] $Mo_2O_3L_2$,[18−21,31−33] $Mo_2O_3L_2(sol)_2$[21] (L = tridentate, sol = solvent), and $Mo_2O_3L_2$ (L = tetradentate)[34] are well known.

In this paper, we report microanalytical, spectroscopic, mass spectrometric, and X-ray diffraction data which show that the purple "oxo-Mo(IV)" complex and its various modifications contain the dinuclear μ-oxo-Mo(V) complex, $Mo^V_2O_3$(L-NS_2)$_2$. The reformulation of this compound reconciles the "unusual" properties of the substance (vide supra) and permits a more complete and accurate description of the Berg−Holm model. This will, in turn, assist efforts to understand and model the structures and functions of the ubiquitous and important oxomolybdoenzymes.[10,24,25]

Results and Discussion

We have prepared and characterized several forms of purple Mo_2O_3(L-NS_2)$_2$. The first was synthesized by reacting MoO_2(L-NS_2) with PPh_3 in dmf followed by precipitation with diethyl ether.[2,3] The second was obtained by reacting MoO_2(L-NS_2) with PPh_3 in 1:10 dmf:$CHCl_3$; in this case, the microcrystalline product precipitated directly from the reaction mixture.[8] The third form, which precipitated when MoO_2(L-NS_2) was reacted with PPh_3 in neat chloroform, has not been reported previously. These three forms are different solvates of Mo_2O_3(L-NS_2)$_2$. A fourth, purple-brown form was obtained by drying each of the above compounds at 80 °C under vacuum. The air-stable compounds are soluble in dmf, sparingly soluble in chlorinated solvents, and insoluble in alcohols and diethyl ether.

The original material (form 1)[2,3] analyzed closely for "MoO(L-NS_2)(dmf)". However, analytical data were also consistent with the formulations Mo_2O_3(L-NS_2)$_2$(dmf)$_2$ and Mo_2O_3(L-NS_2)$_2$·2dmf, the extra half-oxygen per Mo being difficult to detect by elemental analysis. Minor variations in reaction conditions produced samples which analyzed for Mo:dmf ratios in the range from 1:1 to 2:1, consistent with variable levels of lattice solvent. The second form analyzed for the mixed solvate Mo_2O_3(L-NS_2)$_2$·2sol (sol = dmf:10$CHCl_3$). The microanalysis of the form precipitated from neat chloroform was consistent with the formula Mo_2O_3(L-NS_2)$_2$·2$CHCl_3$. The dried compounds analyzed for Mo_2O_3(L-NS_2)$_2$. Although consistent with the microanalytical data, the alternative formulations [Mo^{IV}O(L-NS_2)]$_x$·x(sol) (sol = dmf or $CHCl_3$) are not supported by other data (vide infra). Other solvates, e.g., Mo_2O_3(L-NS_2)$_2$·2CH_2Cl_2, can also be obtained by changing solvent.

The IR spectrum of Mo_2O_3(L-NS_2)$_2$·2dmf is rich in bands due to L-NS_2 and the other ligand and lattice components. A strong band at 945 cm^{-1} has been assigned to the ν(Mo═O) mode of the terminal oxo group of MoO(L-NS_2)(dmf).[2,3] The band, which shifts to 901 cm^{-1} upon ^{18}O-labeling, can now be assigned to the ν_{as}(Mo═O) mode of the *anti*-[$Mo_2O_2(\mu$-O)] unit. A very strong band at 1671 cm^{-1} may be assigned to the ν(C═O) mode of a dmf molecule. This band is only 2 cm^{-1} lower in energy than the corresponding band of neat dmf, consistent with the presence of lattice rather than coordinated dmf. Typically, coordination of dmf results in a ca. 30−40 cm^{-1} lowering in the energy of the ν(C═O) mode.[35] Other bands assignable to lattice dmf occur at 1444, 1087, and 661 cm^{-1}.

(17) The dinuclear structure canvassed in ref 10 is based on the bis-(thiolate)-bridged structure of Zn_2(L-NS_2)$_2$: Kaptein, B.; Wang-Griffin, L.; Barf, G.; Kellogg, R. M. *J. Chem. Soc., Chem. Commun.* **1987**, 1457.

(18) Stiefel, E. I. *Prog. Inorg. Chem.* **1977**, *22*, 1.

(19) (a) Garner, C. D.; Charnock, J. M. In *Comprehensive Coordination Chemistry*; Wilkinson, G., Gillard, R. D., McCleverty, J. A., Eds.; Pergamon: Oxford, 1987; Chapter 36.4, p 1329. (b) Stiefel, E. I. In *Comprehensive Coordination Chemistry*; Wilkinson, G., Gillard, R. D., McCleverty, J. A., Eds.; Pergamon: Oxford, 1987; Chapter 36.5, p 1375.

(20) Craig, J. A.; Harlan, E. W.; Snyder, B. S.; Whitener, M. A.; Holm, R. H. *Inorg. Chem.* **1989**, *28*, 2082.

(21) Stelzig, L.; Kötte, S.; Krebs, B. *J. Chem. Soc., Dalton Trans.* **1998**, 2921.

(22) (a) Newton, W. E.; McDonald, J. W. *J. Less-Common Met.* **1977**, *54*, 51. (b) Chen, G. J.-J.; McDonald, J. W.; Bavard, D. C.; Newton, W. E. *Inorg. Chem.* **1985**, *24*, 2327.

(23) Holm, R. H. *Chem. Rev.* **1987**, *87*, 1401.

(24) Enemark, J. H.; Young, C. G. *Adv. Inorg. Chem.* **1993**, *40*, 1.

(25) Young, C. G. In *Biomimetic Oxidations Catalyzed by Transition Metals*; Meunier, B., Ed.; Imperial College Press: London, 1999; Chapter 9 (in press).

(26) (a) Roberts, S. A.; Young, C. G.; Cleland, W. E., Jr.; Ortega, R. B.; Enemark, J. H. *Inorg. Chem.* **1988**, *27*, 3044. (b) Laughlin, L. J.; Young, C. G. *Inorg. Chem.* **1996**, *35*, 1050.

(27) Oku, H.; Ueyama, N.; Kondo, M.; Nakamura, A. *Inorg. Chem.* **1994**, *33*, 209.

(28) (a) Baird, D. M.; Rheingold, A. L.; Croll, S. D.; DiCenso, A. T. *Inorg. Chem.* **1986**, *25*, 3458. (b) Baird, D. M.; Falzone, S.; Haky, J. E. *Inorg. Chem.* **1989**, *28*, 4561. (c) Baird, D. M.; Aburri, C.; Barron, L. S.; Rodriguez, S. A. *Inorg. Chim. Acta* **1995**, *237*, 117.

(29) Bhattacharjee, S.; Bhattacharyya, R. *J. Chem. Soc., Dalton Trans.* **1993**, 1151. We[25] have speculated that the saturation kinetics reported for the oxidation reactions described indicate the involvement of dinuclear Mo(V) ONS donor thiocarbazate complexes, not mononuclear oxo-Mo(IV) species. This view is supported by recent work on related NS_2 ligand complexes.[21]

(30) Examples include: (a) Ricard, L.; Estienne, J.; Karagiannidis, P.; Toledano, P.; Fischer, J.; Mitschler, A.; Weiss, R. *J. Coord. Chem.* **1974**, *3*, 277. (b) Cotton, F. A.; Fanwick, P. E.; Fitch, J. W., III. *Inorg. Chem.* **1978**, *17*, 3254. (c) Garner, C. D.; Howlader, N. C.; Mabbs, F. E.; McPhail, A. T.; Onan, K. D. *J. Chem. Soc., Dalton Trans.* **1979**, 962. (d) Tatsumisago, M.; Matsubayashi, G.-E.; Tanaka, T.; Nishigaki, S.; Nakatsu, K. *J. Chem. Soc., Dalton Trans.* **1982**, 121. (e) Thompson, R. L.; Lee, S.; Geib, S. J.; Cooper, N. J. *Inorg. Chem.* **1993**, *32*, 6067.

(31) Tsao, Y.-Y. P.; Fritchie, C. J., Jr.; Levy, H. A. *J. Am. Chem. Soc.* **1978**, *100*, 4089.

(32) Hyde, J.; Magin, L.; Vella, P.; Zubieta, J. *Stereodyn. Mol. Syst., Proc. Symp.* **1979**, 227.

(33) Hyde, J. R.; Zubieta, J. *Cryst. Struct. Commun.* **1982**, *11*, 929.

(34) (a) Dahlstrom, P. L.; Hyde, J. R.; Vella, P. A.; Zubieta, J. *Inorg. Chem.* **1982**, *21*, 927. (b) Sellmann, D.; Grasser, F.; Knoch, F.; Moll, M. *Z. Naturforsch.* **1992**, *B47*, 61. (c) Barnard, K. R.; Bruck, M.; Huber, S.; Grittini, C.; Enemark, J. H.; Gable, R. W.; Wedd, A. G. *Inorg. Chem.* **1997**, *36*, 637.

(35) Examples include: (a) Rajan, O. A.; Chakravorty, A. *Inorg. Chem.* **1981**, *20*, 660. (b) Coucouvanis, D.; Toupadakis, A.; Hadjikyriacou, A. *Inorg. Chem.* **1988**, *27*, 3272. (c) Allaire, F.; Beauchamp, A. L. *Inorg. Chim. Acta* **1989**, *156*, 241.

Bands at 765 and 470 cm^{-1} may be assigned to ν_{as}(MoOMo) and δ(MoOMo) modes, respectively.[22,36] The dried dmf solvate exhibits a very similar IR spectrum, except that the strong band at 1671 cm^{-1} is totally absent and the bands at 1444, 1087, and 661 cm^{-1} are diminished considerably (L-NS_2 bands overlap these dmf bands); the ν(Mo═O) band at 945 cm^{-1} shifts to 935 cm^{-1} upon drying. For the compound prepared using 1:10 dmf:$CHCl_3$ as solvent, the dmf bands are markedly less intense, and bands attributable to lattice $CHCl_3$ are present; this is consistent with the mixed solvate indicated by microanalysis. The dmf bands are totally absent from the spectrum of Mo_2O_3-(L-NS_2)$_2$·2$CHCl_3$ which, in addition to bands associated with the complex, exhibits bands due to lattice $CHCl_3$ at 3009, 1222, and 749 cm^{-1} (cf. bands at 3021, 1216, and 760 cm^{-1} for neat $CHCl_3$). These are replaced by bands at 2245, 909, and 730 cm^{-1} in the spectra of samples prepared using $CDCl_3$ as solvent (cf. bands at 2255, 909, and 734 cm^{-1} for neat $CDCl_3$). The $CH(D)Cl_3$ bands are absent from the spectra of the dried compounds, which are identical to the spectrum of the dried dmf solvate; here the ν(Mo═O) band at 939 cm^{-1} shifts to 935 cm^{-1} upon drying.

All forms of Mo_2O_3(L-NS_2)$_2$ crush to produce identical deep-purple colors and dissolve in dmf to produce intense purple solutions with UV−visible spectra exactly matching the spectrum reported for "MoO(L-NS_2)(dmf)";[2,3] these spectra exhibit intense charge-transfer bands at 734 (2430), 528 (12 700), and 365 nm (ϵ 11 900 M^{-1}·cm^{-1}) [ϵ calculated for Mo_2O_3(L-NS_2)$_2$·2dmf]. We note that the stability of the complex in dmf appears to be critically dependent on the purity of the solvent. In contrast, CH_2Cl_2 solutions are much more stable, even for long periods in air. The spectrum in CH_2Cl_2 is qualitatively similar to that in dmf, with bands at 715 (570), 538 (18 000), and 390 nm (ϵ 8500 M^{-1}·cm^{-1}). Solutions in CH_2Cl_2 obey Beer's law, consistent with the absence of a significant equilibrium involving mononuclear oxo-Mo(IV) and dioxo-Mo(VI) species. This conclusion is supported by the observation that MoO_2(L-NS_2) undergoes oxygen exchange with $H_2{}^{18}O$ but that "MoO(L-NS)-(dmf)" does not.[8] Purple colors and UV−visible bands in the 330−380- and 500−520-nm regions are characteristic of six-coordinate μ-oxo-Mo(V) complexes with S_4 and S_2N_2 ligands,[18−20] but few data are available for five-coordinate NS_2 ligand complexes. Recently, however, Stelzig et al.[21] reported bands at 393 and 526 nm in the spectrum of purple Mo_2O_3[2-SC_6H_4C-(Me)NNC(S)NHCPh_3]$_2$, which is qualitatively similar to the spectrum of Mo_2O_3(L-NS_2)$_2$.

The presence of dinuclear Mo_2O_3(L-NS_2)$_2$ (M) in solutions of the compounds was confirmed by electrospray ionization mass spectrometry. Strong peak clusters at *m*/*z* 1245.1 and 1267.1, assignable to $[M + H]^+$ and $[M + Na]^+$ ions, respectively, were observed for all samples examined. The isotope patterns of these two peak clusters precisely matched those calculated. The $[M + Na]^+$ peak cluster and a comparison of the observed and calculated peak cluster for $[M + Na]^+$ are shown in Figure 1. Less intense peak clusters derived from MoO_2(L-NS_2) were also observed as a result of aerial oxidation during sample preparation and analysis. These included peak clusters at *m*/*z* 727.1, 1135.2, and 1157.2, attributable to [MoO_2-(L-NS_2)(dmf) + $Na]^+$, [MoO_2(L-NS(SH))$_2$ + $H]^+$, and [MoO_2-(L-NS(SH))$_2$ + $Na]^+$, respectively. These peaks were also observed in the mass spectrum of pure MoO_2(L-NS_2) in dmf. There was no evidence under any conditions for peaks indicating the existence of MoO(L-NS_2)(dmf), e.g., $[M + H]^+$ *m*/*z* 689 or $[M + Na]^+$ *m*/*z* 711, or species of the type $[MoO(L\text{-}NS_2)]_x$.

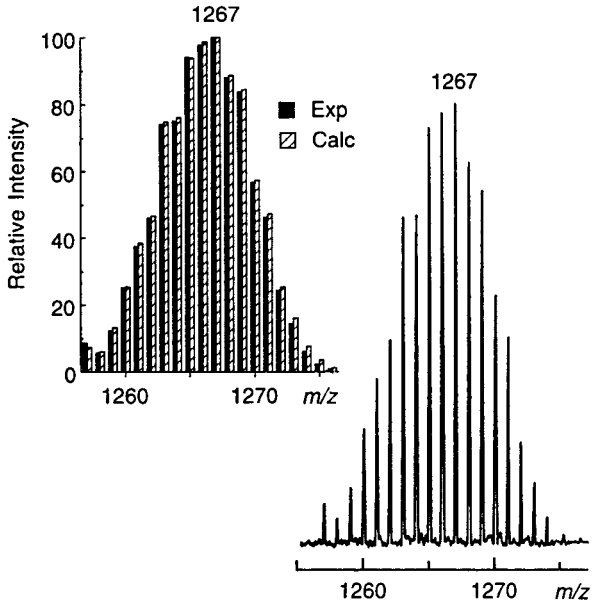

Figure 1. Dominant $[M + Na]^+$ peak cluster in the electrospray ionization mass spectrum of Mo_2O_3(L-NS_2)$_2$·2dmf. The inset on the left shows a comparison of the experimental and calculated isotope patterns for $[M + Na]^+$.

A ^{31}P NMR experiment provided crucial support for the original formulation, i.e., MoO(L-NS_2)(dmf).[2,10] In this experiment, the reaction of MoO_2(L-NS_2) (10 mM) with PPh_3 (1.88 equiv) in anaerobic dmf produced a spectrum exhibiting resonances at δ 43.5 (relative intensity 1.0), 25.9 (6.8), and −4.6 (7.1), which were assigned to MoO(L-NS_2)($OPPh_3$), $OPPh_3$, and PPh_3, respectively. The observed integrated ratio of $OPPh_3$-(total)/PPh_3 = (6.8 + 1)/7.1 = 1.10 was consistent with the value expected for the reaction in eq 2, i.e., 1.0/0.88 = 1.14 ($x \approx 0.13$; only the "dmf adduct" is isolated in syntheses[2,3]).

$$Mo^{VI}O_2(L\text{-}NS_2) + PPh_3 + (1 - x)dmf \rightarrow (1 - x)Mo^{IV}O(L\text{-}NS_2)(dmf) + xMo^{IV}O(L\text{-}NS_2)(OPPh_3) + (1 - x)OPPh_3 \quad (2)$$

Carefully monitored ^{31}P NMR experiments showed that the reaction occurs in two stages. The first stage in the reaction of pure MoO_2(L-NS_2) (ca. 50 mM) with PPh_3 (1.12 equiv) in chloroform under anaerobic conditions was complete in 6−8 h. At this point, resonances at δ 28.2 ($OPPh_3$) and −6.5 (PPh_3) were observed, along with a small resonance at δ 42.4 (ca. 5% of $OPPh_3$ resonance). The integrated $OPPh_3$/PPh_3 ratio of 0.82 was very close to the ratio of 0.80 predicted using eq 3 but very different from that predicted using eqs 1 or 2, i.e., 8.3.

$$2Mo^{VI}O_2(L\text{-}NS_2) + PPh_3 \rightarrow Mo^{V}{}_2O_3(L\text{-}NS_2)_2 + OPPh_3 \quad (3)$$

Further, spiking experiments and literature reports[37] support the assignment of the δ 42.4 resonance (and the δ 43.5 resonance observed previously[2,10]) to $SPPh_3$, not MoO(L-NS_2)($OPPh_3$). The $SPPh_3$ appears to arise from reaction of PPh_3 with the complex-(es) *and* an unidentified impurity in some samples of MoO_2-

(36) The assignment of the ν_{as}(MoOMo) band must be regarded as tentative since strong/medium intensity ligand bands obscure the 800−700-cm^{-1} region. Disappearance of the band at 765 cm^{-1} was the most conspicuous change upon ^{18}O labeling, but the corresponding band of the labeled compound was obscured by ligand bands. The band at 470 cm^{-1} shifted to 460 cm^{-1} in the ^{18}O-labeled compound. Both of the 765- and 470-cm^{-1} bands were absent from the spectrum of MoO_2(L-NS_2).

(37) For example: $SPPh_3$, $\delta(^{31}P)$ −42.6. Maier, L. *J. Inorg. Nucl. Chem.* **1962**, *24*, 1073.

Table 1. Crystallographic Data

	$Mo_2O_3(L\text{-}NS_2)_2\cdot 2dmf$	$Mo_2O_3(L\text{-}NS_2)_2\cdot 2CHCl_3$
formula	$C_{72}H_{68}Mo_2N_4O_5S_4$	$C_{68}H_{56}Cl_6Mo_2N_2O_3S_4$
fw	1389.5	1482.1
cryst syst	monoclinic	monoclinic
space group	$P2_1/n$	$P2_1/c$
a, Å	10.2769(2)	13.6643(5)
b, Å	11.5337(2)	11.2738(4)
c, Å	26.5524(5)	22.0034(7)
β, deg	92.332(1)	106.674(2)
V, Å^3	3144.67(9)	3247.1(2)
Z	2	2
ρ_{calc}, g·cm^{-3}	1.467	1.482
μ, mm^{-1}	0.587	0.809
GOF (on F^2)	1.314	1.325
R[a]	0.054	0.049
R_w[b]	0.053	0.053

[a] $R = \sum||F_o| - |F_c||/\sum|F_o|$. [b] $R_w = [(\sum w(|F_o| - |F_c|)^2/\sum w|F_o|^2)]^{1/2}$.

($L\text{-}NS_2$). At the end of stage one, crystals of $Mo_2O_3(L\text{-}NS_2)_2\cdot 2CDCl_3$ had precipitated from the reaction mixture in near-quantitative yield. In stage two of the reaction, these crystals were consumed with further conversion of PPh_3 to $OPPh_3$, $SPPh_3$ (maximum 20% of $OPPh_3$ resonance), and compounds with ^{31}P resonances at ca. δ 46 and 23.5 (ca. 10% of $OPPh_3$). After many weeks, a brown suspension containing several species was obtained. A similar experiment involving $MoO_2(L\text{-}NS_2)$ (50 mM) and PPh_3 (0.75 equiv) yielded an $OPPh_3/PPh_3$ ratio of 2.1 at the end of stage one (calculated for eq 3, 2.0). During stage two of this experiment, the δ 46 and 23.5 resonances were evident only after several weeks. Reaction of purified $MoO_2(L\text{-}NS_2)$ in d_7-dmf (ca. 50 mM) with 1.09 mol equiv of PPh_3 under anaerobic conditions yielded similar results, with $OPPh_3/PPh_3 = 0.96$ at the end of stage one of the reaction (cf. 0.98 and 11.1 calculated for eqs 3 and 1, 2, respectively). Again, the second stage in the reaction resulted in the full consumption of PPh_3. The reaction of $Mo_2O_3(L\text{-}NS_2)_2$ with PPh_3 is under further investigation.[38]

The crystal structures of $Mo_2O_3(L\text{-}NS_2)_2\cdot 2dmf$ and $Mo_2O_3(L\text{-}NS_2)_2\cdot 2CHCl_3$ were determined as described in Table 1 and the Experimental Section. These structures confirm the presence of the dinuclear μ-oxo-Mo(V) complex and lattice solvent; the structure of the complex in the dmf solvate is displayed in Figure 2, while the complex and solvent interactions present in the chloroform solvate are displayed in Figure 3. Selected bond distances and angles are presented in Table 2. The following discussion applies to both structures (parameters for the chloroform solvate are given in square brackets). The overall structure of the Mo complex involves the bridging of two five-coordinate, trigonal-bipyramidal Mo centers via a common apical μ-oxo ligand, O(2). Atom O(2) resides on an inversion center which relates the two halves of the molecule. The Mo(1)−O(2)−Mo(1)′ bond is linear, the $[Mo_2O_3]$ unit is planar, and the terminal oxo ligands adopt an *anti* disposition.

The trigonal plane is defined by atoms O(1), S(1), and S(2), the apexes of the pyramids by the atoms N(1) and O(2). The

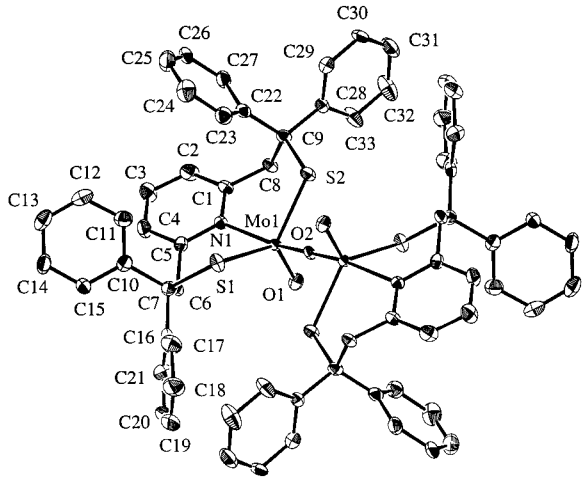

Figure 2. Molecular structure of $Mo_2O_3(L\text{-}NS_2)_2$ in the dmf disolvate.

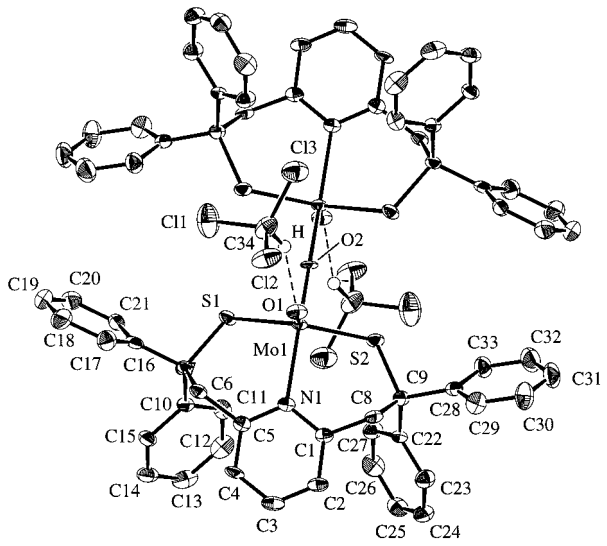

Figure 3. Structure of $Mo_2O_3(L\text{-}NS_2)_2\cdot 2CHCl_3$, showing the arrangement and interactions (as dashed lines) of the complex and the lattice chloroform molecules.

Mo(1) atom lies only 0.02 [0.06] Å out of the equatorial plane toward the N(1) atom. With the exception of O(2), the donor atoms are displaced by less than 0.15 Å from idealized trigonal-bipyramidal positions. The O(2) atom is displaced 0.50 [0.55] Å from its idealized position, and the Mo(1)−O(2) vector makes an angle of ca. 16 [17]° with the 3-fold axis of an idealized trigonal bipyramid. The planes defined by O(1), Mo(1), O(2) and O(1), S(1), S(2) are related by a dihedral angle of 89.7 [88.9]°, close to the ideal angle of 90°. The L−Mo−L angles in the trigonal plane range from 117.6(1) to 124.13(5)°, with an average (in both molecules) of 120°. The L−Mo(1)−N(1) angles range from 88.0(2) to 92.8(2)°, with an average of 91°; the N(1) and Mo(1) atoms lie on the three-fold axis of an idealized trigonal bipyramid. The quite disparate L−Mo(1)−O(2) angles, O(1)−Mo(1)−O(2) = 104.5(2) [105.0(1)]°, S(1)−Mo(1)−O(2) = 81.32(5) [79.98(3)]°, S(2)−Mo(1)−O(2) = 82.89(5) [81.93(3)]°, and N(1)−Mo(1)−O(2) = 163.6(1) [162.2(1)]°, reflect the off-axis position of the bridging O(2) atom. The τ values of 0.72 [0.63] provide a quantitative measure of the distortion away from an ideal trigonal bipyramid (τ 1.0).[39]

The Mo(1)−O(1) and Mo(1)−O(2) distances of 1.681(5) [1.696(4)] and 1.8639(6) [1.8703(4)] Å are typical of terminal

(38) Extended or heated (ca. 60 °C in dmf) reactions of $Mo_2O_3(L\text{-}NS_2)_2$ with PPh_3 result in the formation of a gray-green compound. IR spectra exhibited bands due to lattice dmf (ν(CO) 1673 cm^{-1}) and $L\text{-}NS_2$, but bands due to terminal oxo ligands were absent. Electrospray ionization mass spectra showed a dominant peak cluster at m/z 1251.1, which can be ascribed to an $[Mo_2O_2(L\text{-}NS_2)_2 + Na]^+$ ion pair. These data are consistent with the formulation $Mo^{IV}_2(\mu\text{-}O)_2(L\text{-}NS_2)_2\cdot x$dmf. Preliminary X-ray diffraction analyses support a novel di-μ-oxo-Mo(IV) structure, the structural flexibility of $L\text{-}NS_2$ allowing the close approach (ca. 2.6 Å) of the molybdenum centers. A paramagnetic species, possibly $Mo^{V}OCl(L\text{-}NS_2)$,[9] is one of several products formed when $MoO_2(L\text{-}NS_2)$ reacts with PPh_3 in chlorinated solvents over long periods.

(39) Addison, A. W.; Rao, T. N.; Reedijk, J.; van Rijn, J.; Verschoor, G. C. *J. Chem. Soc., Dalton Trans.* **1984**, 1349.

Table 2. Selected Bond Distances (Å) and Angles (deg) for $Mo_2O_3(L\text{-}NS_2)_2 \cdot 2sol$

	sol			sol			sol	
distance/angle	dmf	$CHCl_3$	distance/angle	dmf	$CHCl_3$	distance/angle	dmf	$CHCl_3$
Mo(1)−O(1)	1.681(5)	1.696(4)	Mo(1)−O(2)	1.8639(6)	1.8703(4)	Mo(1)−S(2)	2.356(2)	2.361(1)
Mo(1)−N(1)	2.287(6)	2.288(4)	Mo(1)−S(1)	2.357(2)	2.355(1)			
O(1)−Mo(1)−O(2)	104.5(2)	105.0(1)	O(1)−Mo(1)−N(1)	91.7(2)	92.8(2)	N(1)−Mo(1)−S(2)	92.1(2)	90.8(1)
O(1)−Mo(1)−S(1)	121.9(2)	118.0(1)	O(1)−Mo(1)−S(2)	117.6(2)	117.7(1)	Mo(1)−O(2)−Mo(1)′	180.00	180.00
O(2)−Mo(1)−N(1)	163.6(1)	162.2(1)	O(2)−Mo(1)−S(1)	81.32(5)	79.98(3)	S(1)−Mo(1)−S(2)	120.50(7)	124.13(5)
O(2)−Mo(1)−S(2)	82.89(5)	81.93(3)	N(1)−Mo(1)−S(1)	88.0(2)	90.91(9)			

and bridging oxomolybdenum units, respectively.[30−34,40−42] The Mo(1)−N(1) distance of 2.287(6) [2.288(4)] Å is consistent with a lengthening induced by the *trans* influence of the bridging oxo ligand.[41] The Mo−S distances are typical for molybdenum−thiolate bonds.[42]

A pseudo-mirror plane bisects each of the L-NS_2 ligands. A slight swivelling of the pyridine ring toward S(2) is reflected in the displacements of N(1) and C(3) from the O(1), Mo(1), O(2) plane by 0.11 [0.04] and 0.38 [0.06] Å, respectively. The magnitude of this distortion appears to be related to the arrangement of lattice solvent molecules. The Mo(1)−O(1) bond is bisected by the plane of the pyridine group, with Mo(1) displaced 0.30 [0.46] Å from the plane. The plane of the pyridine unit is nearly perpendicular to the O(1)−Mo(1)−O(2) plane (dihedral angle = 88 [89]°), and the metallocyclic chelate arms of the ligand adopt boat conformations. The planes defined by Mo(1), S(1), N(1) and Mo, N(1), S(2) have dihedral angles of 58.1 [61.8]° and 62.4 [62.3]°, respectively, with the plane of the $[Mo_2O_3]$ core. The lattice dmf molecules are disordered in hydrophobic sites well removed from the pseudo-mirror plane, with the dmf nitrogen atom ca. 4.4 Å from the terminal oxo group O(1). The voids *trans* to the terminal oxo ligands in the dmf solvate accommodate a phenyl group from a neighboring molecule. In contrast, the lattice chloroform molecules are ordered due to an interaction between solvent C−H and O=Mo groups, characterized by a H···O(1) distance of 2.20 Å and a C−H···O(1) angle of 152° (Figure 3). (Similar interactions between the complex and H^+ or Na^+ in solution may account for the ions observed by mass spectrometry.) The chloroform molecules lie close to the pseudo-mirror plane of the complex and largely reside in the voids *trans* to the second oxo ligand; this accounts for the slightly larger S(1)−Mo(1)−S(2) angle and smaller declination of the N(1)−C(3) vector from the pseudo-mirror plane in the chloroform solvate. The molecular surface of $Mo_2O_3(L\text{-}NS_2)_2$ resembles an oblate ellipsoid with short and long axes of 16 and 18 Å, respectively, and a thickness of only ca. 6 Å. In solution, each face of the molecule would present an oxo group and a phenyl-protected vacant site to the solvent medium.

Many five- and six-coordinate complexes containing the $[Mo_2O_2(\mu\text{-}O)]$ core are known.[18,19,30−34] Here, we restrict our discussion to complexes with structures closely related to that of $Mo_2O_3(L\text{-}NS_2)_2$, viz., $Mo_2O_3[X(C_2H_4S)_2]_2$ [X = (Me)N,[31] S,[32] O[33]] and $Mo_2O_3[2\text{-}SC_6H_4CHNNC(S)NHCPh_3]_2$.[21] These complexes contain five-coordinate, trigonal-bipyramidal Mo centers connected by a bridging oxo group on an inversion center; they exhibit a linear Mo−O−Mo unit, a planar $[Mo_2O_3]$ unit, and an *anti* disposition of the terminal oxo ligands. The $[Mo_2O_3]$ cores of all the compounds are virtually superimposable, with atom displacements (Δ, for the dmf solvate) as follows (Δ(−O−) = 0 Å in each case): for superposition of $Mo_2O_3(L\text{-}NS_2)_2$ and $Mo_2O_3[MeN(C_2H_4S)_2]_2$, Δ(=O) = 0.012 Å, Δ(Mo) = 0.011 Å; for $Mo_2O_3(L\text{-}NS_2)_2$ and $Mo_2O_3[O(C_2H_4S)_2]_2$, Δ(=O) = 0.178 Å, Δ(Mo) = 0.061 Å; for $Mo_2O_3(L\text{-}NS_2)_2$ and $Mo_2O_3[S(C_2H_4S)_2]_2$, Δ(=O) = 0.056 Å, Δ(Mo) = 0.055 Å; for $Mo_2O_3(L\text{-}NS_2)_2$ and $Mo_2O_3[2\text{-}SC_6H_4CHNNC(S)NHCPh_3]_2$, Δ(=O) = 0.065 Å, Δ(Mo) = 0.049 Å. The displacements of the S and O/N donor atoms range from 0.195 to 0.56 Å, with $Mo_2O_3[MeN(C_2H_4S)_2]_2$ showing the closest conjunction of these atoms with those of $Mo_2O_3(L\text{-}NS_2)_2$, viz., Δ(S(1)) = 0.244 Å, Δ(S(2)) = 0.318 Å, Δ(N(1)) = 0.195 Å. Differences in the coordination spheres appear to result primarily from the difference in the chelate ring sizes, which are six-membered in the case of $Mo_2O_3(L\text{-}NS_2)_2$ but five-membered in the other complexes.

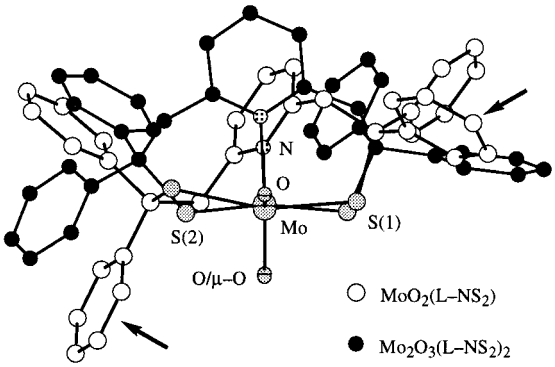

Figure 4. Superposition of the structures of $MoO_2(L\text{-}NS_2)$[2,3] and one-half of $Mo_2O_3(L\text{-}NS_2)_2$ (dmf disolvate) as viewed down the Mo=O vector of the dinuclear complex (the Mo−(μ-O) group lies in the page). The carbon atoms of the L-NS_2 ligands have been differentiated as indicated by the legend (see text for further description).

Examination of the structure of $MoO_2(L\text{-}NS_2)$ led Berg and Holm to conclude that dinucleation via a μ-oxo ligand was prevented by the flanking of the Mo=O units by bulky phenyl groups;[2,3] the possible rearrangement of the ligand to accommodate dinucleation was not canvassed. However, comparison of the structures of $MoO_2(L\text{-}NS_2)$ and one-half of $Mo_2O_3(L\text{-}NS_2)_2$ (dmf solvate) shows that the structural flexibility of L-NS_2 easily accommodates dinucleation (Figure 4). The dioxo complex exhibits a trigonal-bipyramidal structure with O and N donor atoms defining the trigonal plane and apical thiolate sulfur atoms. The projection of the N → Mo vector bisects the O−Mo−O angle, and the plane of the pyridine moiety makes an angle of 61.9° with the MoO_2 plane; the canting of the pyridine ring produces a pseudo-two-fold arrangement of the chelate rings leading to the apical sulfur atoms. The oxo groups are flanked by the phenyl groups indicated by the arrows in Figure 4. In $Mo_2O_3(L\text{-}NS_2)_2$, the N(1) atom has moved toward the terminal oxo group through an arc of ca. 35° to a position *trans* to the μ-oxo group. This is accompanied by a movement of the S(1) and S(2) atoms away from the terminal oxo group

(40) Nugent, W. A.; Mayer, J. M. *Metal−Ligand Multiple Bonds*; Wiley: New York, 1988.
(41) West, B. O. *Polyhedron* **1989**, *8*, 219.
(42) Orpen, A. G.; Brammer, L.; Allen, F. H.; Kennard, O.; Watson, D. G.; Taylor, R. *J. Chem. Soc., Dalton Trans.* **1989**, S1.

through angles of ca. 30° and 16°, respectively, closing the S(1)−Mo−S(2) angle from 156.4(1)° for MoO_2(L-NS_2) to ca. 120° in Mo_2O_3(L-NS_2)$_2$. In the process, the S atoms move marginally toward the μ-oxo ligand, but C(7) and C(9), and the attached phenyl groups, are moved back out of the intermetal region, thus permitting the formation of the dinuclear species. The changes result in a trigonal-bipyramidal structure but one where the O/N and S donor ligands have exchanged roles. The precise orientations of the phenyl groups in the title compounds differ due to small twists about the (S)C−C_{ipso} bonds. Contrary to the original conclusion,[2,3] the *gem* diphenyl groups do not provide the steric bulk necessary to prevent comproportionation and dinucleation.[38]

Conclusion

This work demonstrates that the compound previously characterized as $Mo^{IV}O$(L-NS_2)(dmf) is the dmf disolvate of $Mo^V_2O_3$(L-NS_2)$_2$ formed by comproportionation of MoO_2(L-NS_2) and the immediate product of OAT, viz., MoO(L-NS_2). Contrary to previous claims,[2−10] comproportionation and dinucleation reactions are not suppressed by the L-NS_2 ligand, and the OAT chemistry of this system cannot be described in terms of mononuclear Mo(VI) and Mo(IV) complexes. The observation that these[2−8] and other[28] dinuclear Mo(V) complexes can support two-electron OAT reactions, including the reduction of biological substrates such as dimethyl sulfoxide and nitrate, indicates that redox equivalents need not be localized on a single metal or redox center. In this regard, the behavior of these dinuclear Mo(V) species may find parallels in the "electronic buffer" [43] and "gating" [44] functions of molybdopterin and the possible redox role of Se−S moieties in some molybdenum enzymes.[45]

A number of other systems have been developed as synthetic models for mononuclear oxomolybdoenzyme active sites.[24,25] These include pyrazolylborate systems which feature extensive OAT and coupled proton−electron transfer (CEPT) reactions involving mononuclear complexes spanning biologically important oxidation states (VI, V, and IV) and core−ligand sets.[26,46] Comproportionation reactions are also a feature of these systems, but biologically relevant mononuclear Mo(V) complexes, rather than dinuclear species, are usually generated.[46] These systems are unique in closely mimicking the OAT/CEPT turnover chemistry of the enzymes, albeit with nonbiological coligands. Other successful OAT models include those based on bis(4-*tert*-butylphenyl)-2-pyridylmethanethiolate(1−),[11−13] 2,2-diphenyl-2-mercaptoethanoate(2−),[47] and (various) dithiolene[14−16,27,48] ligand complexes. In the mercaptoethanoate and dithiolene systems, the mononuclearity of the component anionic complexes appears to be electrostatically rather than sterically enforced. OAT reactions spanning des-oxo-Mo(IV) and oxo-Mo(VI) species with dithiolenic coligands define a new and exciting chapter in the modeling of bis(pterin) oxomolybdoenzymes such as dimethyl sulfoxide reductase.[16]

Experimental Section

Materials and Methods. The ligand, H_2(L-NS_2), and MoO_2(L-NS_2) were prepared by literature methods.[3] Oxygen-18-labeled compounds were prepared from $Mo^{18}O_2$(L-NS_2), generated in situ in dmf, by exchange with $H_2{}^{18}O$.[8] Reactions and solution studies were performed under dinitrogen using dried, deoxygenated solvents and Schlenk techniques. The products of the reactions may be filtered and washed in air, and then dried in vacuo, without detectable decomposition. Solid-state (KBr disk) infrared spectra were recorded on a Bio-Rad FTS 165 FTIR spectrophotometer. $^{31}P\{^1H\}$ NMR spectra were recorded using Varian Unity 300- and 400-MHz spectrometers. Mass spectra were recorded on a Bruker BioApex 47e FTMS fitted with an Analytica electrospray source operating with a capillary voltage of 120 V. The compounds were initially dissolved in dmf and then diluted with dmf/CH_2Cl_2/MeOH (1:1:2) (for the μ-oxo compounds) or neat dmf (for MoO_2(L-NS_2)) and introduced into the source by direct infusion (syringe pump) at a rate of 70 μL/h. UV−visible spectra were recorded on an Hitachi 150-20 double-beam spectrophotometer. Microanalyses were performed by Atlantic Microlabs Inc. (Norcross, GA).

Mo_2O_3(L-NS_2)$_2$·2dmf. The compound and its ^{18}O-labeled analogue were synthesized by the method described previously for "MoO(L-NS_2)(dmf)".[3]

Anal. Calcd for $C_{72}H_{68}Mo_2N_4O_5S_4$: C, 62.23; H, 4.93; N, 4.03; S, 9.25. Found: C, 61.74; H, 4.99; N, 4.19; S, 8.98. IR (KBr): 3055w, 3009w, 2927w, 1671vs, 1604m, 1575w, 1490m, 1457m, 1444m, 1385w, 1257w, 1224w, 1180w, 1087m, 1017w, 944s, 770sh, 746s, 699s, 662w, 597w, 567w, 510w, 470w, 421w cm^{-1}.

Mo_2O_3(L-NS_2)$_2$·2(dmf:10$CHCl_3$). Following the briefly described literature method,[8] a mixture of MoO_2(L-NS_2) (500 mg, 0.79 mmol) and PPh_3 (312 mg, 1.19 mmol) in 1:10 dmf:$CHCl_3$ (22 mL) was stirred for 48 h. The purple microcrystalline solid was isolated by filtration and washed with ice-cold chloroform. Yield: 300 mg, 53%.

Anal. Calcd for $C_{66.36}H_{57.1}Cl_{5.45}Mo_2N_{2.18}O_{3.18}S_4$: C, 55.72; H, 3.90; N, 2.07; S, 8.70. Found: C, 55.28; H, 3.88; N, 2.12; S, 8.46. IR (KBr): 3057w, 3009w, 2944w, 1671w, 1604m, 1575w, 1489m, 1458m, 1444m, 1385w, 1325w, 1263w, 1222m, 1178w, 1125w, 1083w, 1033w, 1018w, 999w, 940s, 797w, 749s, 697s, 664w, 597w, 586w, 570w, 509w, 479w, 423w cm^{-1}.

Mo_2O_3(L-NS_2)$_2$·2$CHCl_3$. A mixture of MoO_2(L-NS_2) (500 mg, 0.79 mmol) and PPh_3 (312 mg, 1.19 mmol) in chloroform (20 mL) was stirred for 24 h. The purple microcrystalline solid was isolated by filtration and washed with ice-cold chloroform. Yield: 426 mg, 60%.

Anal. Calcd for $C_{68}H_{56}Cl_6Mo_2N_2O_3S_4$: C, 55.11; H, 3.80; N, 1.89; S, 8.65; Cl, 14.35. Found: C, 55.26; H, 3.75; N, 1.83; S, 8.77; Cl,

(43) Westcott, B. L.; Gruhn, N. E.; Enemark, J. H. *J. Am. Chem. Soc.* **1998**, *120*, 3382.

(44) (a) Inscore, F. E.; McNaughton, R.; Westcott, B. L.; Helton, M. E.; Jones, R.; Dhawan, I. K.; Enemark, J. H.; Kirk, M. L. *Inorg. Chem.* **1999**, *38*, 1401. (b) Jones, R. M.; Inscore, F. E.; Hille, R.; Kirk, M. L. *Inorg. Chem.*, in press.

(45) (a) George, G. N.; Colangelo, C. M.; Dong, J.; Scott, R. A.; Khangulov, S. V.; Gladyshev, V. N.; Stadtman, T. C. *J. Am. Chem. Soc.* **1998**, *120*, 1267. (b) George, G. N.; Costa, C.; Moura, J. J. G.; Moura, I. *J. Am. Chem. Soc.* **1999**, *121*, 2625.

(46) (a) Xiao, Z.; Young, C. G.; Enemark, J. H.; Wedd, A. G. *J. Am. Chem. Soc.* **1992**, *114*, 9194. (b) Xiao, Z.; Bruck, M. A.; Doyle, C.; Enemark, J. H.; Grittini, C.; Gable, R. W.; Wedd, A. G.; Young, C. G. *Inorg. Chem.* **1995**, *34*, 5950. (c) Cleland, W. E., Jr.; Barnhart, K. M.; Yamanouchi, K.; Collison, D.; Mabbs, F. E.; Ortega, R. B.; Enemark, J. H. *Inorg. Chem.* **1987**, *26*, 1017. (d) Xiao, Z.; Gable, R. W.; Wedd, A. G.; Young, C. G. *J. Am. Chem. Soc.* **1996**, *118*, 2912. (e) Xiao, Z.; Bruck, M. A.; Enemark, J. H.; Young, C. G.; Wedd, A. G. *Inorg. Chem.* **1996**, *35*, 7508. (f) Xiao, Z.; Bruck, M. A.; Enemark, J. H.; Young, C. G.; Wedd, A. G. *J. Biol. Inorg. Chem.* **1996**, *1*, 415.

(47) (a) Sanz, V.; Picher, T.; Palanca, P.; Gómez-Romero, P.; Llopis, E.; Ramirez, J. A.; Beltrán, D.; Cervilla, A. *Inorg. Chem.* **1991**, *30*, 3113. (b) Cervilla, A.; Corma, A.; Fornés, V.; Llopis, E.; Palanca, P.; Rey, F.; Ribera, A. *J. Am. Chem. Soc.* **1994**, *116*, 1595. (c) Cervilla, A.; Llopis, E.; Ribera, A.; Corma, A.; Fornés, V.; Rey, F. *J. Chem. Soc., Dalton Trans.* **1994**, 2953. (d) Corma, A.; Rey, F.; Thomas, J. M.; Sankar, G.; Greaves, G. N.; Cervilla, A.; Llopis, E.; Ribeira, A. *J. Chem. Soc., Chem. Commun.* **1996**, 1613.

(48) Examples include: (a) Das, S. K.; Chaudhury, P. K.; Biswas, D.; Sarkar S. *J. Am. Chem. Soc.* **1994**, *116*, 9061. (b) Ueyama, N.; Oku, H.; Kondo, M.; Okamura, T.; Yoshinaga, N.; Nakamura, A. *Inorg. Chem.* **1996**, *35*, 643. (c) Oku, H.; Ueyama, N.; Nakamura A. *Inorg. Chem.* **1997**, *36*, 1504. (d) Collison, D.; Garner, C. D.; Joule, J. A. *Chem. Soc. Rev.* **1996**, 25. (e) Davies, E. S.; Beddoes, R. L.; Collison, D.; Dinsmore, A.; Docrat, A.; Joule, J. A.; Wilson, C. R.; Garner, C. D. *J. Chem. Soc., Dalton Trans.* **1997**, 3985. (f) Davies, E. S.; Aston, G. M.; Beddoes, R. L.; Collison, D.; Dinsmore, A.; Docrat, A.; Joule, J. A.; Wilson, C. R.; Garner, C. D. *J. Chem. Soc., Dalton Trans.* **1998**, 3647.

14.25. IR (KBr): 3058w, 3009w, 2944w, 1604m, 1575w, 1489m, 1458m, 1444m, 1325w, 1263w, 1222m, 1177w, 1125w, 1083w, 1033w, 1018w, 999w, 939s, 797w, 749vs, 697s, 664w, 597w, 586w, 570w, 508w, 480w, 423w cm^{-1}.

$Mo_2O_3(L\text{-}NS_2)_2$. The compounds above were dried at 80 °C under vacuum for 6 h. A color change from purple to dark brown-purple was observed, but the solid crushed purple and produced purple solutions with the UV−visible spectrum previously ascribed to $MoO(L\text{-}NS_2)(dmf)$.[2,3] Microanalyses were consistent with the formation of $Mo_2O_3(L\text{-}NS_2)_2$, e.g., for the compound obtained by drying $Mo_2O_3(L\text{-}NS_2)_2\cdot 2CHCl_3$.

Anal. Calcd for $C_{66}H_{54}Mo_2N_2O_3S_4$: C, 63.76; H, 4.38; N, 2.25; S, 10.32; Cl, 0.00. Found: C, 63.15; H, 4.32; N, 2.26; S, 10.16; Cl, 0.00. IR (KBr, from all sources): 3055w, 3021w, 2940w, 1602m, 1574w, 1489m, 1445m, 1386w, 1327w, 1256w, 1224w, 1175w, 1120w, 1082w, 1034w, 1017w, 935s, 792w, 766m, 747m, 698s, 663w, 596w, 587w, 567w, 511w, 469w, 423w cm^{-1}.

Reaction Stoichiometry. The samples of $MoO_2(L\text{-}NS_2)$ employed in the following experiments were recrystallized five times from dichloromethane (containing a few drops of Me_2SO) by the addition of methanol. The reaction stoichiometry was established by ^{31}P NMR experiments performed under strictly anaerobic conditions using carefully dried and deoxygenated solvents. Assignment of the resonance at δ ca. 43 to $SPPh_3$ was confirmed by NMR spiking and thin-layer chromatographic studies. Two examples follow.

(A) A solution of $MoO_2(L\text{-}NS_2)$ (17.73 mg, 2.819×10^{-5} mol) and PPh_3 (8.30 mg, 3.168×10^{-5} mol) in $CDCl_3$ (0.6 mL) was monitored by ^{31}P NMR for 4 weeks (every hour for 1 day, then less frequently). Precipitation of purple crystals of $Mo_2O_3(L\text{-}NS_2)_2\cdot 2CDCl_3$ (identified spectroscopically) began shortly after mixing and was complete after 6−8 h. Due to their relatively low density, the crystals can be induced to float, permitting clean ^{31}P NMR spectra of the mother liquor to be recorded. Integration of the PPh_3 (δ −6.5) and $OPPh_3$ (δ 28.2) resonances gave an $OPPh_3/PPh_3$ ratio of 0.82. No phosphorus could be detected in the crystalline product isolated from the reaction mixture.

(B) A solution of $MoO_2(L\text{-}NS_2)$ (20.71 mg, 3.29×10^{-5} mol) and PPh_3 (9.44 mg, 3.60×10^{-5} mol) in d_7-dmf (0.6 mL) was monitored by ^{31}P NMR as above. After stage one of the reaction, integration of the PPh_3 and $OPPh_3$ resonances gave an $OPPh_3/PPh_3$ ratio of 0.96. Continuation of the experiment led to the complete conversion of PPh_3 to $OPPh_3$ and $SPPh_3$.

Crystallography. Purple crystals of $Mo_2O_3(L\text{-}NS_2)_2\cdot 2dmf$ were grown by slow diffusion of diethyl ether into a 2-mL portion of the $MoO_2(L\text{-}NS_2)/PPh_3$/dmf reaction mixture from the literature synthesis.[3] Red-purple crystals of $Mo_2O_3(L\text{-}NS_2)_2\cdot 2CHCl_3$ were grown by modifying the synthetic procedure above such that crystallization took place from the undisturbed reaction mixture.

Crystallographic data were collected at 123(1) K on an Enraf-Nonius Kappa CCD diffractometer system equipped with graphite-monochromated Mo Kα radiation (λ = 0.710 73 Å) using ϕ rotations with 1° frames, detector-to-crystal distances of 35 and 30 mm, and detector 2θ offsets of −16° and −11° for $Mo_2O_3(L\text{-}NS_2)_2\cdot 2dmf$ and $Mo_2O_3(L\text{-}NS_2)_2\cdot 2CHCl_3$, respectively. The final unit cell determinations, scaling of the data, and corrections for Lorentz and polarization effects were performed with DENZO-SMN.[49] Analytical absorption corrections were applied using the XPREP[50] routine. The structures were solved by direct methods (SIR92[51]), expanded with the Fourier technique and refined by the full-matrix least-squares technique using the crystal structure analysis package teXsan[52] on a Silicon Graphics Indy computer.

All of the non-hydrogen atoms of the molybdenum complex were located in the initial solution and were refined anisotropically. The hydrogen atoms of the complex were included in the refinement at their calculated, geometrically constrained positions. Examination of the difference map for $Mo_2O_3(L\text{-}NS_2)_2\cdot 2dmf$ revealed that the dmf of crystallization was positionally disordered. It could not be modeled in terms of identifiable, partially occupied dmf molecules but was modeled as follows: a well-resolved peak in the midst of a diffuse region of electron density was assigned as a nitrogen atom and refined isotropically. Six peaks of high electron density were within reasonable bonding distances of the nitrogen, and these were assigned as carbon atoms and refined isotropically with the sum of their site occupancy factors constrained to three. An additional well-resolved peak at the periphery of the diffuse region of electron density was assigned as an oxygen atom and refined isotropically. The chloroform of crystallization in $Mo_2O_3(L\text{-}NS_2)_2\cdot 2CHCl_3$ was not disordered. Crystallographic data are summarized in Table 1, and selected interatomic distances and angles are given in Table 2. Figures 2 and 3 were prepared using ORTEP,[53] with thermal ellipsoids drawn at the 50% probability level (hydrogens omitted for clarity).

Acknowledgment. We thank Ms. Sally Duck, Monash University, for obtaining electrospray ionization mass spectrometric data and Dr. Gary Fallon, Monash University, for access to the diffractometer and for helpful discussions. We gratefully acknowledge the financial support of the Australian Research Council.

Supporting Information Available: An X-ray crystallographic file, in CIF format, is available on the Internet only. See any current masthead page for ordering information and Web access instructions.

JA9900959

(49) Otwinowski, Z.; Minor, W. In *Methods in Enzymology*; Carter, C. W., Jr., Sweet, R. M., Eds.; Academic: San Diego, CA, 1997; Vol. 276, p 307.

(50) XPREP, Version 5.03/486, Siemens Analytical X-ray Instruments, Inc., Madison, Wisconsin, 1990−4.

(51) Altomare, A.; Cascarano, G.; Giacovazzo, C.; Burla, M. C.; Polidori, G.; Camalli, M. *J. Appl. Crystallogr.* **1994**, *27*, 435.

(52) teXsan: Single-Crystal Structure Analysis Software, Version 1.7, Molecular Structure Corp., The Woodlands, TX, 1992−1997.

(53) Johnson, C. K. ORTEP; Report ORNL-5138, Oak Ridge National Laboratory, Oak Ridge, TN, 1976.